Distinct G protein–coupled receptor recycling pathways allow spatial control of downstream G protein signaling

Shanna Lynn Bowman, Daniel John Shiwarski, and Manojkumar A. Puthenveedu

Department of Biological Sciences, Carnegie Mellon University, Pittsburgh, PA 15213

G protein–coupled receptors (GPCRs) are recycled via a sequence-dependent pathway that is spatially and biochemically distinct from bulk recycling. Why there are two distinct recycling pathways from the endosome is a fundamental question in cell biology. In this study, we show that the separation of these two pathways is essential for normal spatial encoding of GPCR signaling. The prototypical β-2 adrenergic receptor (B2AR) activates Gα stimulatory protein (Gαs) on the endosome exclusively in sequence-dependent recycling tubules marked by actin/sorting nexin/retromer tubular (ASRT) microdomains. B2AR was detected in an active conformation in bulk recycling tubules, but was unable to activate Gαs. Protein kinase A phosphorylation of B2AR increases the fraction of receptors localized to ASRT domains and biases the downstream transcriptional effects of B2AR to genes controlled by endosomal signals. Our results identify the physiological relevance of separating GPCR recycling from bulk recycling and suggest a mechanism to tune downstream responses of GPCR signaling by manipulating the spatial origin of G protein signaling.

Introduction

G protein–coupled receptors (GPCRs) transduce the majority of signals in the human body. Activated receptors are removed from the cell surface by clathrin-mediated endocytosis (von Zastrow and Kobilka, 1992; Lamb et al., 2001; Yoburn et al., 2004; Hanyaloglu and von Zastrow, 2008; Soohoo and Puthenveedu, 2013). Endocytosed GPCRs are transported to the endosome, from where they are either recycled back to the cell surface or degraded in the lysosome (Lefkowitz et al., 1997; Hanyaloglu and von Zastrow, 2008; Marchese et al., 2008; von Zastrow and Williams, 2012).

GPCR recycling requires specific sequences on the receptors and multiple interacting proteins (Hanyaloglu and von Zastrow, 2008; Romero et al., 2011; Magalhaes et al., 2012). Many other proteins that recycle as part of the bulk membrane flow without apparent sequence requirements or interactions (Mayor et al., 1993; Maxfield and McGraw, 2004). Furthermore, sequence-dependent recycling of GPCRs is mediated by tubular microdomains that are spatially and biochemically distinct from the tubular domains that mediate bulk recycling on the same endosome (Puthenveedu et al., 2010). Previous work has defined how GPCRs are sorted into sequence-dependent recycling domains (Puthenveedu et al., 2010; Temkin et al., 2011). Why GPCRs need a specialized recycling pathway, however, is not clear.

The role of endocytic trafficking has been redefined by data indicating that GPCRs can signal from endosomes (Tsvetanova et al., 2015; West and Hanyaloglu, 2015). Although endosomal signaling has been well appreciated for some GPCRs, such as parathyroid hormone receptors (Okazaki et al., 2008; Calebiro et al., 2009; Ferrandon et al., 2009; Werthmann et al., 2012), recent evidence suggests that this might be a general paradigm for GPCRs, as canonical GPCRs like β-2 adrenergic receptors (B2ARs) might also signal through G proteins on the endosome (Irannejad et al., 2013). A conformation-specific nanobody biosensor that recognizes the nucleotide-free form of the Gα stimulatory protein (Gαs) showed that B2AR can support active exchange of G proteins on endosomes (Irannejad et al., 2013). Furthermore, optogenetically engineered production of cAMP, the second messenger downstream of Gαs, at endosomes induced the expression of distinct gene targets compared with cAMP production at the plasma membrane, suggesting that the site of signal origin determines specific downstream consequences (Tsvetanova and von Zastrow, 2014).

In this study, we asked whether sequence-dependent endosomal microdomains play a role in coordinating endosomal signaling. We show that endosomal G protein signaling is restricted to actin/sorting nexin/retromer tubular (ASRT) endosomal microdomains. PKA phosphorylation of B2AR on its C-terminal tail increases the proportion of B2AR localized to ASRT microdomains and generates an endosomal bias in B2AR signaling, increasing transcription of genes specifically

Correspondence to Manojkumar A. Puthenveedu: map3@andrew.cmu.edu

Abbreviations used: ASRT, actin/sorting nexin/retromer tubular; B2AR, β-2 adrenergic receptor; Epac, exchange protein activated by cAMP; FRET, Forster resonance energy transfer; Gαs, Gα stimulatory protein; GPCR, G protein–coupled receptor; TIRF, total internal reflection fluorescence; TUBB, β-tubulin.

The Rockefeller University Press $30.00
J. Cell Biol. Vol. 214 No. 7 797–806
www.jcb.org/cgi/doi/10.1083/jcb.201512068

controlled by endosome-derived cAMP. Our results reveal a physiological reason for why separate recycling pathways evolved for signaling receptors and nutrient receptors.

Results and discussion

We first asked whether B2AR endosomal signaling was restricted to functional tubular domains. We directly quantitated agonist-induced redistribution of B2AR between endosomal microdomains in living cells in real time using live-cell confocal fluorescence microscopy in HEK 293 cells stably expressing fluorescently tagged B2AR. We and others have confirmed that this system accurately reflects the trafficking and signaling of B2AR (Kobilka, 1995; Seachrist et al., 2000; Yudowski et al., 2009; Puthenveedu et al., 2010; Han et al., 2012; Vistein and Puthenveedu, 2013). B2AR localized to the cell surface before addition of the B2AR agonist, isoproterenol (iso; Fig. 1 A). 5-min incubation with iso caused endocytosis and redistributed B2ARs to endosomes (Fig. 1 A). Within endosomal membranes, B2AR localized to tubular structures—previously characterized as ASRT domains that mediate sequence-dependent recycling—that are biochemically distinct from tubules that mediate constitutive recycling (Puthenveedu et al., 2010; Vistein and Puthenveedu, 2013). PKA inhibition increased the percentage of B2AR endosomes with more than one B2AR tubule (Fig. 1 A and Fig. S1 A), consistent with B2AR sorting into both ASRT domains and constitutive tubules (Puthenveedu et al., 2010; Vistein and Puthenveedu, 2013).

To estimate the proportion of B2ARs that localized to ASRT domains, we measured B2AR colocalization with established biochemical markers of these domains: coronin, cortactin, and sorting nexin 1 (SNX1; Puthenveedu et al., 2010; Temkin et al., 2011). 5 min after iso addition, virtually all B2AR tubular domains colocalized with coronin (Fig. 1, B and C) and SNX1 (Fig. 1, D and E), indicating that B2AR was sorted primarily into ASRT domains. After PKA inhibition with the drug KT5720 (KT), ∼50% of B2AR tubular domains were devoid of coronin and SNX1 (Fig. 1, B–E; and Fig. S1, B and C). We observed a similar redistribution away from ASRT domains when two PKA target sites, S345 and S346, on the C-terminal tail of B2AR were mutated to alanine (SS>AA), consistent with published data that PKA phosphorylation restricts B2AR to ASRT domains (Fig. 1, F–H; and Fig. S1, D and E; Vistein and Puthenveedu, 2013). This PKA phosphorylation-mediated relocation of B2AR provided us with an experimental setup to test the functional relevance of B2AR sorting to ASRT domains.

To test whether B2AR endosomal signaling could be spatially resolved in the context of endosomal microdomains, we used a GFP-tagged nanobody biosensor, Nb80, that recognizes the agonist-activated conformation of B2AR (Westfield et al., 2011; Irannejad et al., 2013). Nb80 was recruited to B2AR endosomes 5 min after iso stimulation (Fig. 2 A), consistent with previous data that B2ARs exist in an active conformation at endosomes (Irannejad et al., 2013). Nb80 localized to all domains of the endosome that contained B2AR, including the ASRT microdomains and constitutive tubules containing SS>AA (Fig. 2, B and C; and Fig. S2 A), suggesting that B2AR is in an active conformation in all regions of the endosome, irrespective of whether B2AR was sorted to sequence-dependent or constitutive recycling tubules. As a direct readout of where Gαs was active, we used GFP-tagged Nb37, a nanobody that recognizes the nucleotide-free form of Gαs (Irannejad et al., 2013). In contrast to Nb80, Nb37 localized to punctate regions on the endosome at the base of B2AR recycling tubules (Fig. 2, D and E). Nb37 localization was largely restricted to domains containing the ASRT domain marker cortactin (Fig. 2, E and F; and Fig. S2 B). Interestingly, Nb37 was still localized only to ASRT domains in SS>AA endosomes, even when active receptors were partitioned to both ASRT domains and constitutive tubules were not marked by ASRT components (Fig. 2 E). 50% of the SS>AA tubules were devoid of both Nb37 and cortactin markers (Fig. 2 F and Fig. S2 B). The distinct localization patterns of the nanobodies that detect active receptor and active Gαs indicate that Gαs activation is restricted to ASRT domains, even though B2AR may be in an active conformation in a broader region of the endosome.

To confirm that phosphorylation of B2AR at S345 and S346 confines Gαs activation to ASRT domains, we generated a phosphomimetic version of B2AR, mutating both S345 and S346 to aspartic acid (SS>DD). SS>DD localized exclusively to ASRT domains (Fig. 3 A). Importantly, unlike wild-type B2AR, PKA inhibition did not redistribute SS>DD into constitutive tubules (Fig. 3, A and B), suggesting that phosphorylation of S345 and S346 directly regulates the sorting of B2AR into ASRT domains. Nb37 was recruited only to B2AR and to SS>DD domains overlapping with cortactin (Fig. 3, C and D; and Fig. S2 B), together suggesting that B2ARs, when phosphorylated at S345 and S346, are sorted into ASRT domains, where they activate Gαs. ASRT domains therefore might function as specific scaffolds for recruiting G proteins to the endosome.

Emerging data indicate that production of cAMP signaling at the endosome and the cell surface have distinct downstream effects, as they activate the transcription of different sets of downstream genes (Tsvetanova and von Zastrow, 2014). Based on our data that Nb37 was not recruited to constitutive recycling tubules (Fig. 2, D–F), we hypothesized that the strength of endosomal G protein signaling could be controlled by the dynamic relocation of B2AR to constitutive recycling tubules. To test this, we measured total cAMP response in conditions where B2AR localized exclusively to ASRT domains or to bulk recycling domains. We used a Forster resonance energy transfer (FRET)–based sensor (DiPilato et al., 2004; Ponsioen et al., 2004), which measures cAMP-induced conformational changes in exchange proteins activated by cAMP (Epac's), to resolve cAMP production over time. When cells expressing this sensor and either B2AR or SS>AA were exposed to iso, cAMP levels increased within 2 min. This increase was sustained over 25 min, and B2AR endocytosis was visible within 2 min of iso stimulation in the same cells (Fig. 4, A and B). Total cAMP increased significantly for both B2AR and SS>AA to a similar degree 20 min after iso (Fig. 4 C), indicating that the SS>AA was fully competent to signal through cAMP, comparable to B2AR.

To test whether endosome-specific cAMP responses were regulated by PKA-mediated B2AR relocation, we used reverse transcription followed by quantitative real-time PCR to measure the expression of three genes—PCK1 (phosphoenolpyruvate carboxykinase 1), CGA (glycoprotein hormones, α-polypeptide), and NR4A1 (nuclear receptor subfamily 4 group A member 1)—that are induced specifically by endosomal cAMP (Tsvetanova and von Zastrow, 2014). We isolated RNA from HEK 293 cells stably expressing wild-type B2AR or SS>AA and measured the expression of PCK1 as well as the reference gene, β-tubulin (TUBB). Dose–response curve analysis showed

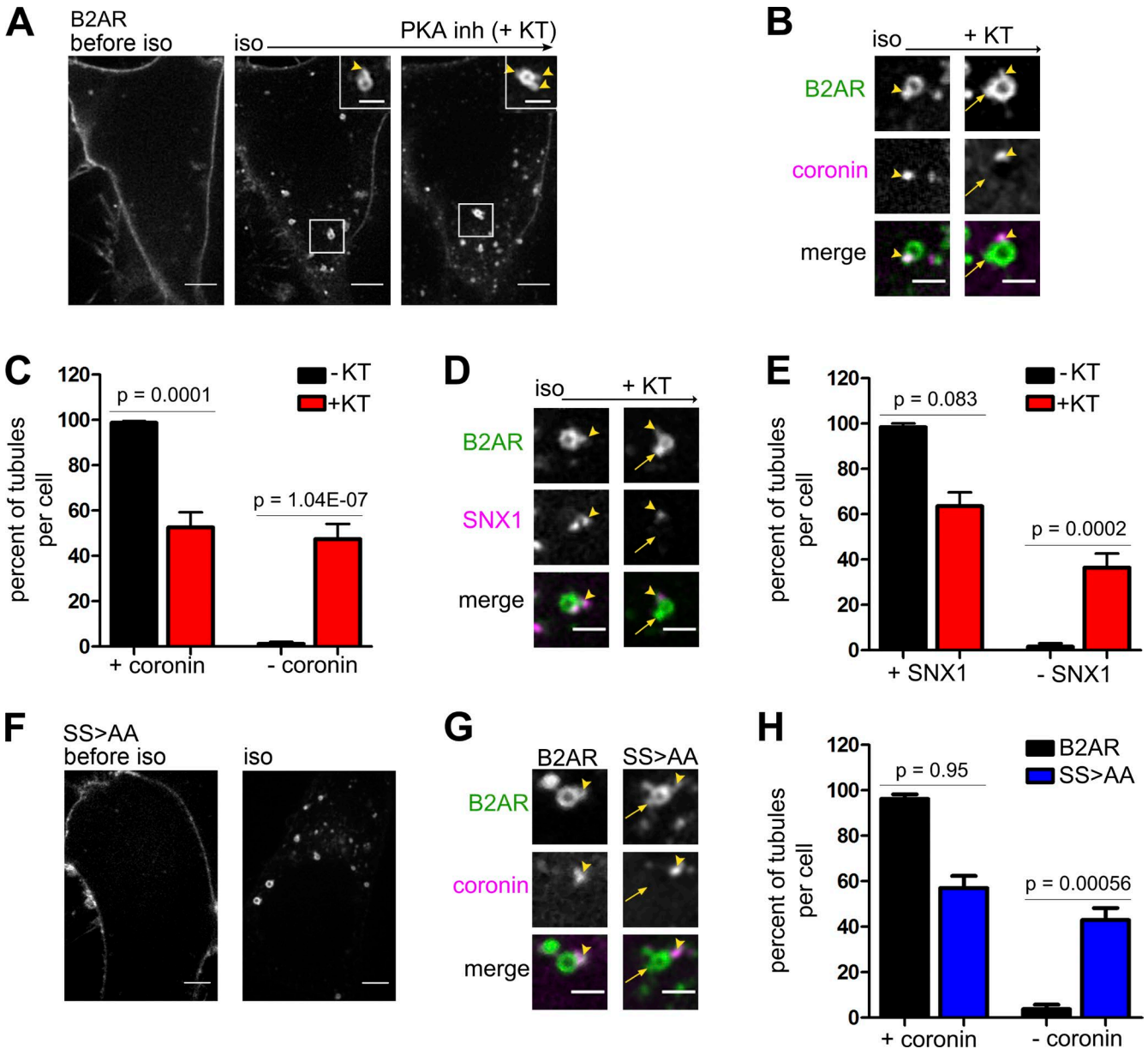

Figure 1. **B2AR phosphorylation at S345 and S346 restricts B2AR to ASRT endosomal microdomains.** (A) Images of iso-induced B2AR endocytosis and PKA inhibition. Before iso, B2ARs localize to the cell surface. 5 min after iso, B2AR redistributes to endosomes and is sorted into tubules (arrowheads). KT was added 5 min after iso. Bars: (main images) 5 µm; (insets) 2 µm. (B) Example images of B2AR and coronin (ASRT marker) with iso and KT. KT causes B2AR to enter non-ASRT domains. (C) Quantitation of percent B2AR in ASRT and non-ASRT tubules. $n = 31$ (–KT, iso) and 14 (KT) cells. (D) Example images of B2AR and SNX1 (ASRT marker) with iso and KT. (B and D) Arrowheads show B2AR in ASRT domains, and arrows show B2AR in non-ASRT domains. Bars, 2 µm. (E) Quantitation of the percent B2AR in ASRT and non-ASRT tubules. $n = 11$ (–KT, iso only) and 18 (+KT, PKA inhibited) cells. (F) 5 min after iso, SS>AA also localized to endosomes and tubules. Bars, 5 µm. (G) Example images of B2AR and SS>AA with coronin. SS>AA localizes to both ASRT domains (arrowheads) and constitutive tubules (arrows). Bars, 2 µm. (H) Quantitation of percent B2AR and SS>AA ASRT tubules. SS>AA localizes to both ASRT and non-ASRT tubules. $n = 13$ (B2AR) and 14 (SS>AA) cells. Error bars in all graphs are SEM across cells.

that TUBB expression changed in a similar concentration-dependent manner with and without iso treatment (Fig. S3, D and E), making it a suitable gene to normalize the expression of iso-dependent genes across treatments. When normalized to TUBB expression, PCK1, CGA, and NR4A1 expression levels increased by approximately five-, six-, and eightfold upon B2AR activation by iso (Fig. 5, A–C).

We then used three independent methods to block receptor endocytosis: dynasore and Dyngo-4a, two inhibitors of dynamin-dependent endocytosis (Macia et al., 2006; Harper et al., 2013; McCluskey et al., 2013), and expression of the dominant-negative mutant of dynamin, dynamin K44A (Herskovits et al., 1993; Damke et al., 1994). All of these ablated the iso-induced increase in PCK1 expression, showing that it required receptor endocytosis (Fig. 5 A; Tsvetanova and von Zastrow, 2014). As a control, pretreatment with Dyngo-4a did not cause a significant decrease in iso-induced whole-cell cAMP levels as measured by the Epac sensor (Fig. S3 C). These results support the model that, although the majority of overall cAMP is derived from initial activation of receptors on the cell surface at this time point, endosome-derived cAMP is a functionally distinct pool (Tsvetanova and von Zastrow, 2014).

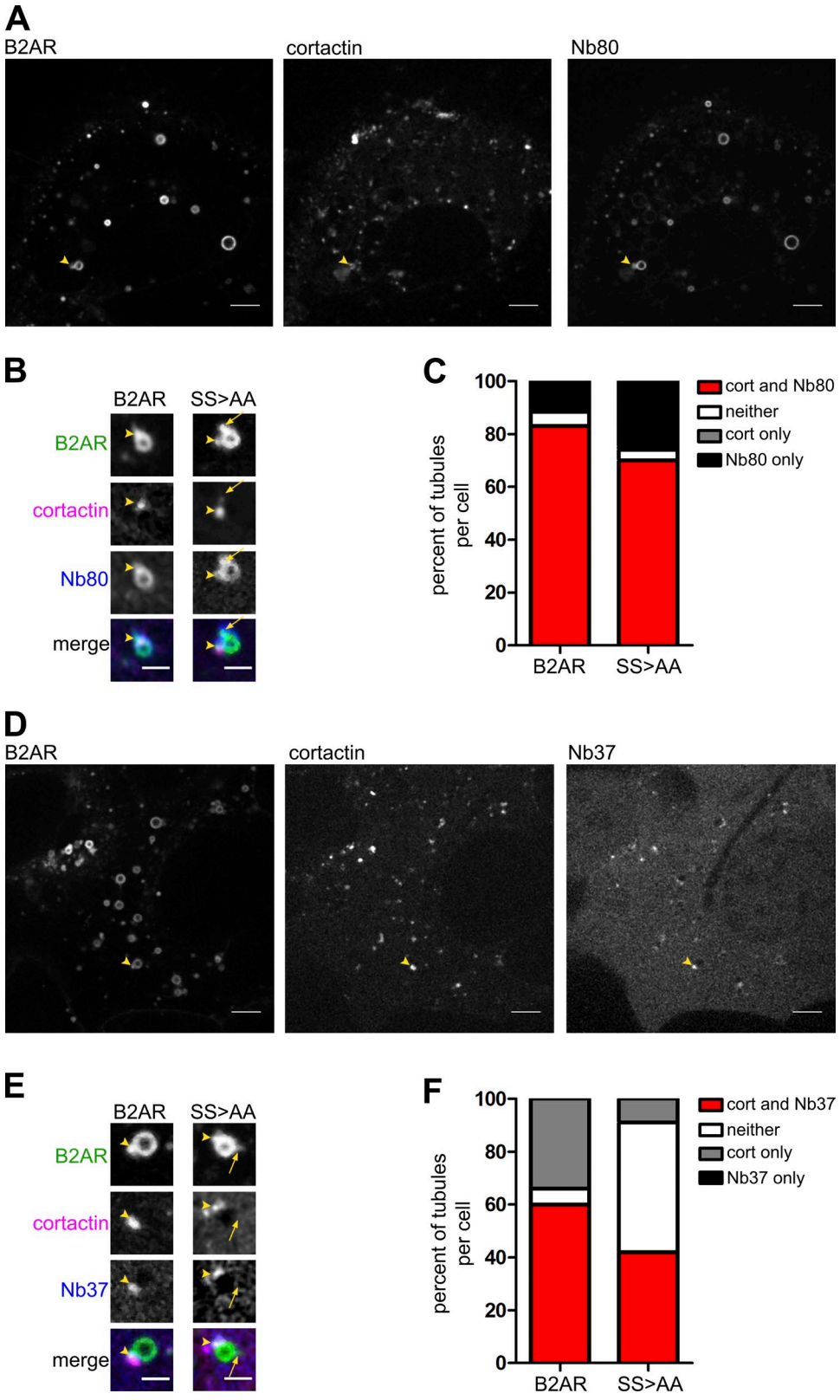

Figure 2. **B2AR activates Gαs exclusively in ASRT endosomal microdomains.** (A) Example images of B2AR, an ASRT marker; cortactin; and Nb80. Nb80 localizes to endosomes and tubules (arrowheads). Bars, 5 µm. (B) Example images of B2AR and SS>AA with cortactin and Nb80. Nb80 localizes to ASRT (arrowheads) and non-ASRT SS>AA tubules (arrows). Bars, 2 µm. (C) Percent tubules per cell with cortactin and Nb80, cortactin or Nb80 only, or neither. n = 15 (B2AR) and 21 (SS>AA) cells. (D) Example images of B2AR, cortactin, and Nb37. Nb37 localizes exclusively to the base of B2AR tubules (arrowheads) with cortactin (ASRT). Bars, 5 µm. (E) Example images of B2AR and SS>AA with cortactin and Nb37. Nb37 is not recruited to SS>AA constitutive tubules (arrows). Arrowheads show B2AR in ASRT domains. Bars, 2 µm. (F) Quantitation of the percentage of total tubules per cell that contain cortactin and Nb37, cortactin or Nb37 only, or neither. n = 42 (B2AR) and 43 (SS>AA) cells.

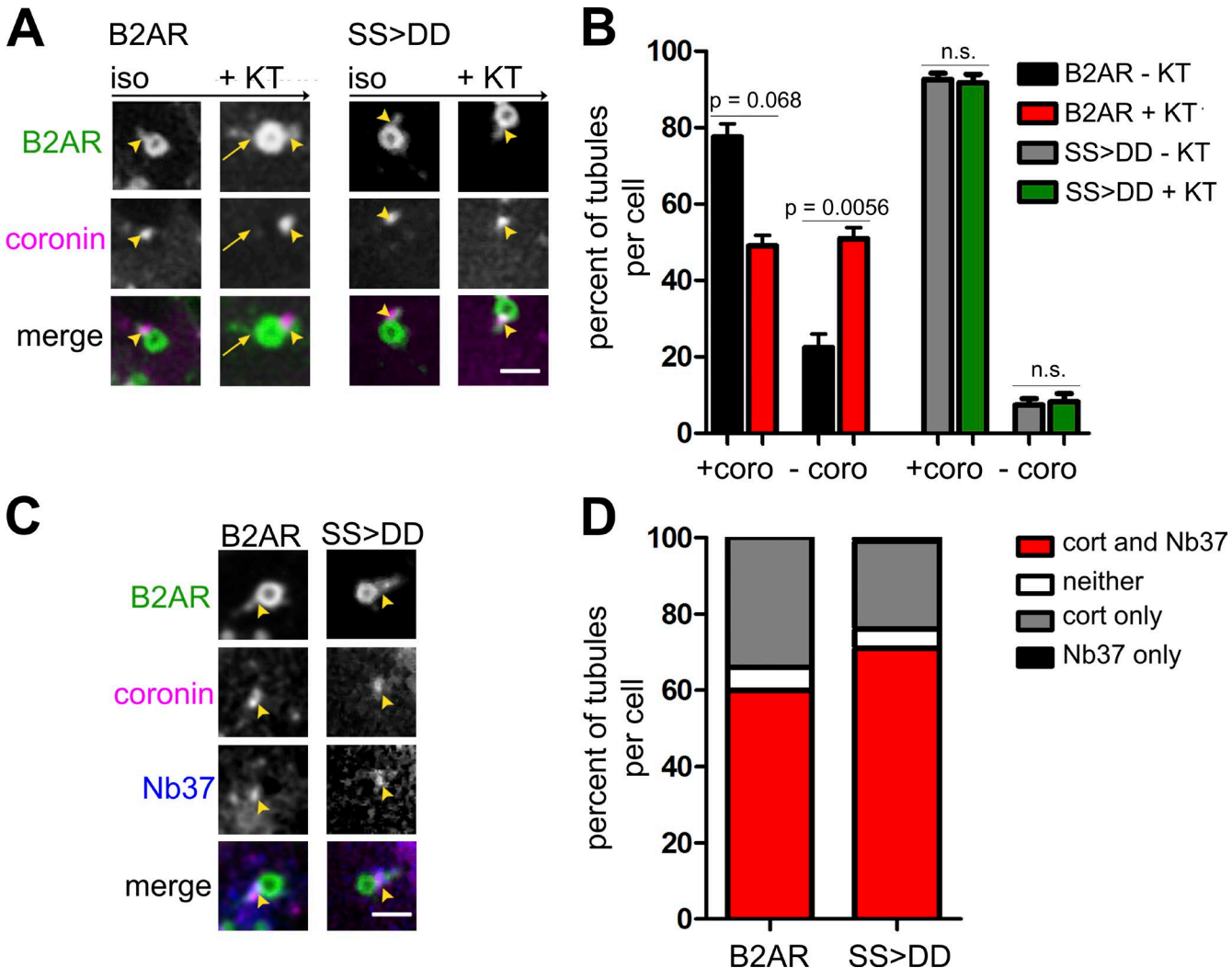

Figure 3. **A phosphomimetic B2AR mutant is restricted to ASRT domains independent of PKA and activates Gαs in ASRT domains.** (A) Example images of B2AR and SS>DD ASRT (arrowheads) and non-ASRT (arrows) tubules after iso and before and after KT. Bar, 2 µm. (B) Percent ASRT tubules (marked by coronin) and non-ASRT tubules for B2AR and SS>DD with and without KT. KT does not cause SS>DD to enter non-ASRT tubules. *n* = 43 (B2AR – KT), 26 (B2AR + KT), 64 (SS>DD – KT), and 36 (SS>DD + KT) cells. n.s., not significant. (C) Example images of FLAG-B2AR and SS>DD with cortactin and Nb37 after iso. Nb37 is recruited to SS>DD ASRT tubules (arrowheads). Bar, 2 µm. (D) Percent tubules per cell that contain cortactin and Nb37, cortactin or Nb37 only, or neither marker. *n* = 42 (B2AR) and 47 (SS>DD) cells. Error bars in all graphs are SEM across cells.

Disruption of ASRT domains by latrunculin A (latA), an actin-depolymerizing agent, ablated the iso-induced increase in PCK1 expression (Fig. 5 A), suggesting that localization of B2AR to ASRT domains was required for induction of PCK1 expression. Addition of latA with iso to B2AR-expressing cells did not significantly change total cAMP produced 20 min after iso (Fig. S3 C), and internalization of B2AR was unaffected when cells were treated with iso and latA (Fig. S3, A and B). Iso-induced increases in CGA and NR4A1 expression were also dependent on endocytosis and intact ASRT domains (Fig. 5, B and C).

We next tested whether PCK1, CGA, and NR4A1 expression is regulated by partitioning B2AR between ASRT and bulk recycling microdomains. To do this, we used SS>AA, the B2AR mutant that cannot be phosphorylated on S345/S346 by PKA and is not restricted from entering bulk tubules. Strikingly, SS>AA activation did not increase expression of endocytosis-dependent genes (Fig. 5, D–F), indicating that SS>AA does not sustain endosomal Gαs signaling to the same degree as wild-type B2AR. Furthermore, the SS>DD phosphomimetic mutant increased the expression of PCK1, CGA, and NR4A1 comparable to the wild-type receptor (Fig. 5, D–F), strongly supporting our model that phosphorylation-dependent sorting of B2AR into ASRT domains facilitates B2AR endosomal Gαs signaling. These results, together with our data that total cAMP levels are not significantly different between B2AR and SS>AA (Fig. 4 C), support the emerging model that endosomal cAMP might be a small but specialized pool of cAMP that has distinct downstream effects on gene activation.

Together, our data reveal a physiological reason for why two separate recycling pathways—sequence-dependent recycling for signaling receptors and bulk recycling for nutrient receptors—have evolved. We show that, although both pathways can support recycling of B2AR (Vistein and Puthenveedu, 2013), only the sequence-dependent pathway can support Gαs signaling from the endosome (Fig. S3 F). This might be the primary role of sequence-dependent recycling. The extent of B2AR partitioning between these two pathways is regulated by the phosphorylation state of a specific PKA target sequence on

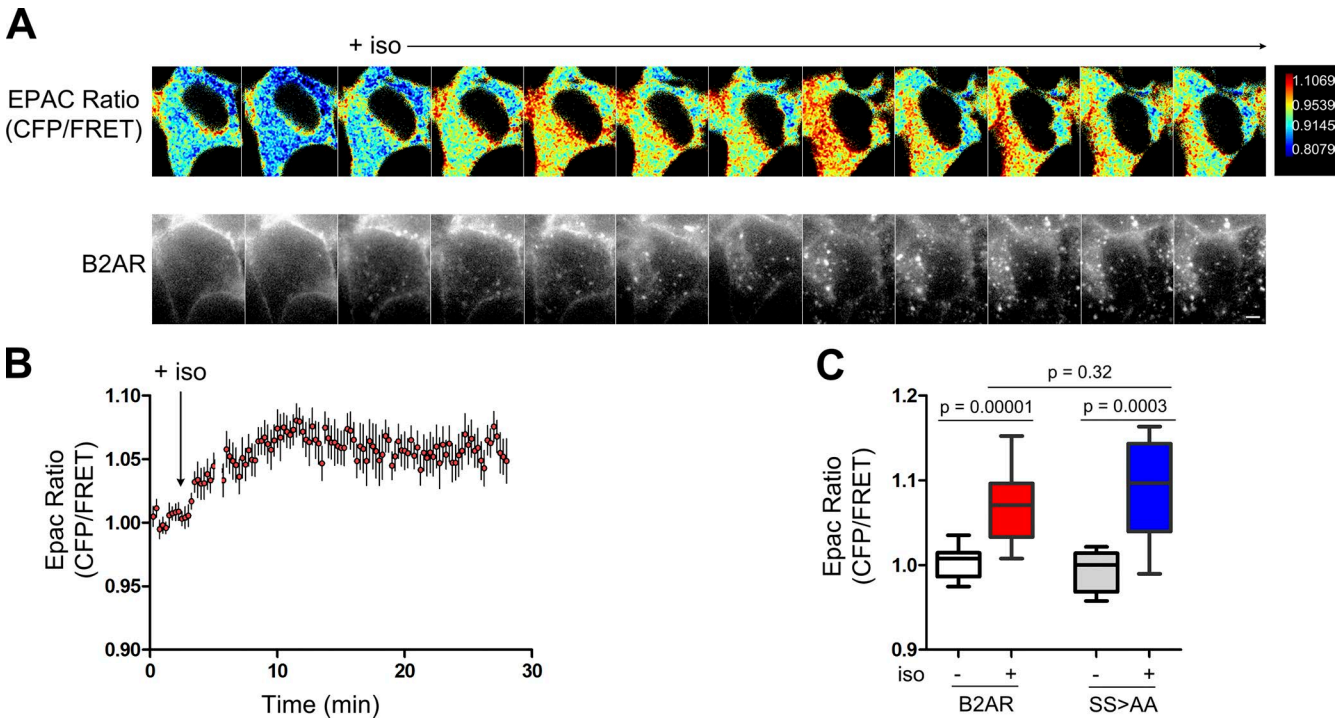

Figure 4. **The localization of B2AR to ASRT or bulk recycling domains does not influence global cAMP levels.** (A) Example images of Epac and B2AR. 1–2 min after iso, the CFP/FRET ratio increases as cAMP is produced and FRET decreases. Bar, 10 µm. (B) CFP/FRET ratio across multiple B2AR cells. Error bars are SEM across cells. *n* = 10 cells. (C) The total cAMP produced at 20 min increased significantly for both B2AR and SS>AA. Data are Tukey box plots from 13 (B2AR) and 10 (SS>AA) cells.

B2AR. This is a control point that determines the spatial bias of adrenergic signaling between surface and endosomal signals, and therefore the downstream complement of genes (Fig. S3 F). PKA is a major target of B2AR itself (Cassel and Selinger, 1978; Gilman, 1987; Lefkowitz, 2007), so this regulation might be a homeostatic mechanism that switches the pattern of downstream consequences based on whether there is a continued presence of agonists. Persistent adrenergic signals, by keeping B2AR in a phosphorylated state, might bias toward endosomal signals, whereas intermittent signals might bias toward surface signals by B2AR dephosphorylation, relocation to bulk tubules, and/or attenuation of endosomal Gαs signaling. This bias might also be controlled differentially by distinct agonists that activate PKA to various degrees. PKA activity is also regulated by other receptors, many of which are coexpressed and often coactivated in neurons and cardiac myocytes (Lefkowitz et al., 1997; Pierce et al., 2002; Gainetdinov et al., 2004; Lefkowitz, 2007), providing a potential mechanism for signaling cross talk.

Our results suggest that the availability of G proteins, and not receptor activation, is the limiting factor for signaling from the endosome. Although B2AR was in an active conformation on the entire endosome, based on Nb80 localization, G protein signaling, detected by Nb37, was restricted to ASRT domains. ASRT domains, in addition to their known roles in stabilizing sequence-dependent tubules and in sorting B2AR into these domains, could also serve as scaffolds to concentrate Gαs proteins, to be activated by B2AR. Interestingly, B2AR can couple to Gαi under some circumstances (Xiao et al., 1995; Daaka et al., 1997; Xiao, 2001), and this could be regulated by PKA phosphorylation (Clark et al., 1989; Hausdorff et al., 1989; Liggett et al., 1989; Okamoto et al., 1991; Seibold et al., 2000; Zamah et al., 2002). There are two separate PKA phosphorylation sites on B2AR: one at S261 and S262, and another at S345 and S346. Although the precise contributions of these sites have not been separated, G protein coupling seems to be primarily regulated by S261/S262 (Clark et al., 1989; Hausdorff et al., 1989; Yuan et al., 1994). Consistent with the global cAMP changes seen in these studies, it is possible that S261/S262 regulates G protein coupling at the plasma membrane, whereas S345/S346 plays an analogous role on the endosome.

Spatial encoding of signals by membrane microdomains suggests that a primary role of membrane trafficking is to move GPCRs between signaling complexes. For example, B2AR may transfer from Gαs signaling to arrestin-mediated signaling in clathrin-coated pits at the plasma membrane, and later to a spatially discrete Gαs signaling complex in endosomal microdomains. Interestingly, in contrast to the activation seen with B2AR, localization of parathyroid hormone receptors to ASRT domains leads to termination of sustained cAMP signaling (Feinstein et al., 2011). Because many GPCRs can signal from endosomes using multiple downstream factors (Okazaki et al., 2008; Calebiro et al., 2009; Ferrandon et al., 2009; Werthmann et al., 2012; Jean-Alphonse et al., 2014), microdomain localization is likely a general mechanism for regulating GPCR signaling, although the specific mechanisms might therefore vary between GPCRs. In any case, the efficiency of receptor partitioning between, and time spent in, distinct complexes might contribute significantly to the tuning of downstream effects separated in space and time. Identifying the molecular mechanisms involved in regulating endosomal sorting of GPCRs could provide candidates to manipulate receptor localization and generate strategies to spatially bias GPCR signaling in the future.

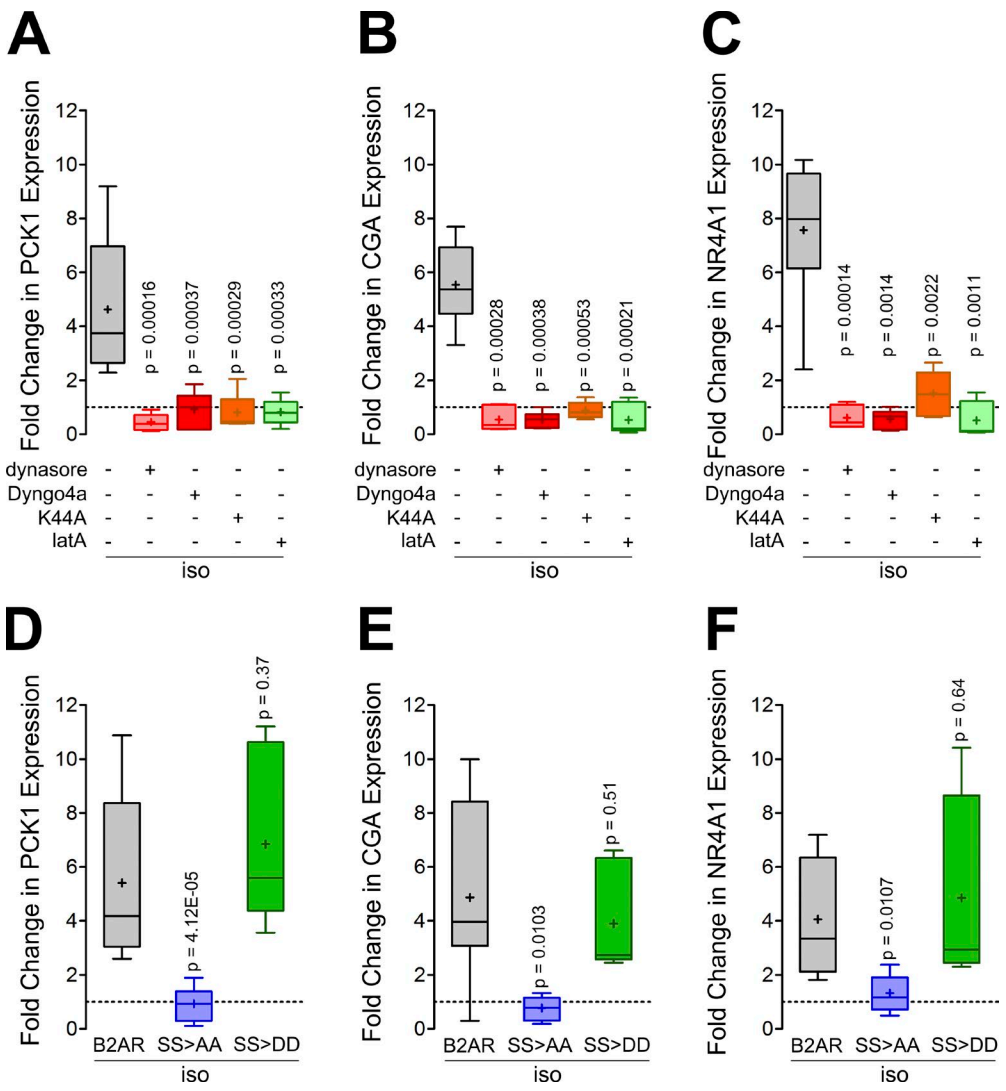

Figure 5. **B2AR localization to ASRT domains correlates with expression of endosomal cAMP-specific genes.** (A–C) Tukey box plots of fold change in PCK1 (A), CGA (B), and NR4A1 (C) expression across multiple experimental replicates. Iso increased PCK1 expression. Dynasore, Dyngo-4a, dynamin-K44A, or latA prevented the iso-induced increase in PCK1 expression. n = 11 for iso, iso + dynasore, and iso + latA, and n = 6 for all others. (D–F) Fold change in PCK1 (D), CGA (E), and NR4A1 (F) expression with iso for B2AR, SS>AA, and SS>DD. Iso increased PCK1 expression for B2AR and SS>DD, but not for SS>AA. n = 14 for B2AR and SS>AA, and n = 6 for SS>DD. Dashed lines throughout indicate the location of value 1 on the y axis. In all cases, p-values in relation to iso treatment alone are shown.

Materials and methods

Constructs and reagents

FLAG-B2AR (B2AR), FLAG-B2AR S345–S346A (SS>AA), cortactin-DsRed, coronin-GFP, SNX1-GFP, and Epac CFP/YFP FRET sensor constructs have been described previously (DiPilato et al., 2004; Hanyaloglu et al., 2005; Puthenveedu et al., 2010; Temkin et al., 2011; Vistein and Puthenveedu, 2013). FLAG-B2AR S345-6D (SS>DD) was created using the QuickChange site-directed mutagenesis protocol and Pfu Turbo polymerase (Agilent Technologies). Nb80- and Nb37-GFP plasmid constructs were gifts from R. Irannejad (University of California, San Francisco, San Francisco, CA) and M. von Zastrow (University of California, San Francisco, San Francisco, CA) and were described previously (Irannejad et al., 2013). HEK 293 cells were obtained from ATCC and maintained in DMEM high glucose (Thermo Fisher Scientific) + 10% FBS (Gibco). Cells were transfected with Effectene (QIAGEN) according to the manufacturer's instructions. Stable cell lines of FLAG-B2AR and FLAG-B2AR S345–S346A were generated with Zeocin (Invitrogen) selection. FLAG-B2AR SS>DD experiments were performed in transiently transfected cells and were assayed 48–96 h after transfection. Cells were passed to a 25-mm coverglass 1 d after transfection with actin or retromer markers, or with the Epac FRET sensor, and imaged 48–96 h after transfection.

Iso hydrochloride (Sigma-Aldrich) was prepared as a 10-mM stock in water, and KT (Santa Cruz Biotechnology, Inc.) was prepared as a 10-mM stock in DMSO. LatA (Cayman Chemical) was prepared at a concentration of 100 µg/ml in ethanol. These drugs were used at a final concentration of 10 µM. Dynasore hydrate was prepared fresh for each experiment, dissolved in DMSO, and used at a final concentration of 80 µM. Dyngo-4a was dissolved in DMSO and used at a final concentration of 30 µM.

Microscope image acquisition and analysis

Confocal images were acquired with a spinning disk system (Andor Revolution XD) on an inverted microscope (Eclipse T*i*; Nikon) equipped with a temperature-, humidity-, and CO_2-controlled chamber

and 60× or 100× 1.49 NA total internal reflection fluorescence (TIRF) objectives (Nikon). Images were acquired on an electron-multiplying charge-coupled device camera (iXon+ 897) using the Andor IQ software (Andor Technology). Cells were imaged live at 37°C in Leibovitz's L15-no phenol red (Gibco) with 1% FBS. Solid-state 488-nm, 561-nm, or 647-nm lasers served as light sources. HEK 293 cells stably expressing FLAG-B2AR were labeled for 10 min at 37°C in DMEM high glucose + 10% FBS with M1 anti-FLAG conjugated to Alexa Fluor 647 (Molecular Probes). Cells were imaged 5–15 min after the addition of iso and 2–5 min after the addition of KT. Stacks and time-lapse images were collected as TIFF images and analyzed with ImageJ (National Institutes of Health). Tubules and actin spots per endosome were counted blindly with scrambled file names. All fluorescence measurements and quantitations were performed on images acquired directly from the camera without adjustments. Simple statistical analyses were performed in Excel (Microsoft) and Prism (GraphPad Software). P-values were generated from unpaired Student's *t* tests.

cAMP measurements with Epac CFP/YFP FRET sensor

Iso-induced cAMP production was measured in live cells with the Epac CFP/YFP FRET sensor (DiPilato et al., 2004; Ponsioen et al., 2004). The Epac sensor contained a CFP (405-nm excitation and 470-nm emission) and YFP (515-nm excitation and 530-nm emission). After cAMP binding to Epac's cAMP-binding domain, a decrease in the FRET signal (CFP excitation at 405 nm and YFP emission at 530 nm) occurred, allowing cAMP production to be measured as a decrease in FRET, which was expressed as the CFP/FRET ratio. CFP and YFP images were acquired, in addition to images of anti-FLAG–Alexa Fluor 647–labeled FLAG-B2AR at 37°C, every 15 s in wide-field excitation using a 60× 1.49 NA TIRF objective (Nikon). Image analysis was performed in ImageJ. For Epac experiments with the drug Dyngo-4a, images were acquired using confocal fluorescence microscopy, rather than wide-field TIRF excitation, to prevent detection of autofluorescence produced by Dyngo-4a. HEK 293 cells stably expressing FLAG-B2AR or FLAG-B2AR–SS>AA were treated with 30 µM Dyngo-4a only, or pretreated for 15 min before addition of 10 µM iso. In latA experiments, cells were treated with 10 µM iso and 10 µM latA simultaneously and imaged. CFP/FRET ratios were normalized to the mean of all time points before iso addition. The pre-iso time point (Fig. 4 C and Fig. S3 C) was 2.5 min before iso addition.

RNA isolation, reverse transcription, and quantitative, real-time PCR

RNA was harvested from HEK 293 cells 2 h after iso addition using the RNeasy Plus Mini kit (QIAGEN) according to the manufacturer's instructions. Cells were cotreated with latA and iso for 2 h. Cells were pretreated with 80 µM dynasore or 30 µM Dyngo-4a for 20 min and then treated with iso for 2 h before RNA isolation. For dynamin K44A experiments, cells were transfected with dynamin K44A-GFP 48 h before RNA isolation. RNA was treated with amplification-grade DNase I (Thermo Fisher Scientific), and reverse transcription was performed with the Superscript First Strand System for RT-PCR (Thermo Fisher Scientific). RNA was amplified using random hexamer primers (Thermo Fisher Scientific). cDNA was then treated with RNase H (Thermo Fisher Scientific) before quantitative PCR reactions. Primers for gene targets were chosen to amplify targets 50–100 bp and spanning an exon–exon junction. The following primers were used to amplify gene targets: TUBB forward (5′-GTGGTACGGAAGGAGGTCGATG-3′) and reverse (5′-AAG GTGACTGCCATCTTGAGG-3′); PCK1 forward (5′-CTGCCCAAG ATCTTCCATGT-3′) and reverse (5′-CAGCACCCTGGAGTTCTC TC-3′); CGA forward (5′-TTCGGATCCACAGTCAACCG-3′) and reverse (5′-ATCCATGGCGCTCCTTTCTC-3′); and NR4A1 forward (5′-GACGGGATAATGTGGTTGGC-3′) and reverse (5′-GGCATC TCACTCTGGATGGA-3′). TUBB was chosen as the reference gene for normalization because its expression did not change significantly with iso addition (Fig. S3). SYBR green Select Master Mix (Thermo Fisher Scientific) was used for quantitative RT-PCR amplification and detection on a BioRad Cfx RT-PCR machine (Bio-Rad Laboratories).

Online supplemental material

Fig. S1 shows supporting data that PKA inhibition increases the number of B2AR tubules per endosome and shows the raw number of tubules per cell with ASRT markers, corresponding to the normalized data in Fig. 1. Fig. S2 shows the number of tubules per cell with ASRT markers, corresponding to the normalized data in Figs. 2 and 3. In relation to Fig. 4, Fig. S3 shows that latA addition with iso does not significantly alter B2AR endocytosis or the iso-dependent increase in cAMP and that pretreatment with Dyngo-4A does not significantly alter iso-induced cAMP production. In relation to Fig. 5, Fig. S3 shows that TUBB expression is not significantly altered by iso and is therefore a suitable reference gene for normalization. Fig. S3 also suggests a model for how spatial encoding of B2AR signaling can create a bias toward endosomal or cell surface signaling responses. Online supplemental material is available at http://www.jcb.org/cgi/content/full/jcb.201512068/DC1.

Acknowledgments

We thank Drs. A. Soohoo and R. Vistein for essential help and comments, Drs. J. Steyaert, M. von Zastrow, and R. Irannejad for nanobodies and helpful comments, and Dr. A.P. Mitchell, Dr. C. Woolford, and K. Lagree for essential help with the quantitative RT-PCR studies. We thank Drs. A. Hanyaloglu, P. Friedman, G. Romero, A. Bisello, J.-P. Vilardaga, A. Linstedt, and T. Lee for reagents, comments, and helpful discussions.

S.L. Bowman was partially supported by a T32 grant from the National Institute of Neurological Disorders and Stroke via the University of Pittsburgh Center for Neuroscience (NS007433), and D.J. Shiwarski was supported by a DeVries Fellowship. M.A. Puthenveedu was supported by National Science Foundation grant 1517776 and National Institutes of Health grant GM117425.

The authors declare no competing financial interests.

Submitted: 19 December 2015
Accepted: 12 August 2016

References

Calebiro, D., V.O. Nikolaev, M.C. Gagliani, T. de Filippis, C. Dees, C. Tacchetti, L. Persani, and M.J. Lohse. 2009. Persistent cAMP-signals triggered by internalized G-protein-coupled receptors. *PLoS Biol.* 7:e1000172. http://dx.doi.org/10.1371/journal.pbio.1000172

Cassel, D., and Z. Selinger. 1978. Mechanism of adenylate cyclase activation through the beta-adrenergic receptor: catecholamine-induced displacement of bound GDP by GTP. *Proc. Natl. Acad. Sci. USA.* 75:4155–4159. http://dx.doi.org/10.1073/pnas.75.9.4155

Clark, R.B., J. Friedman, R.A. Dixon, and C.D. Strader. 1989. Identification of a specific site required for rapid heterologous desensitization of the β-adrenergic receptor by cAMP-dependent protein kinase. *Mol. Pharmacol.* 36:343–348.

Daaka, Y., L.M. Luttrell, and R.J. Lefkowitz. 1997. Switching of the coupling of the β_2-adrenergic receptor to different G proteins by protein kinase A. *Nature.* 390:88–91. http://dx.doi.org/10.1038/36362

Damke, H., T. Baba, D.E. Warnock, and S.L. Schmid. 1994. Induction of mutant dynamin specifically blocks endocytic coated vesicle formation. *J. Cell Biol.* 127:915–934. http://dx.doi.org/10.1083/jcb.127.4.915

DiPilato, L.M., X. Cheng, and J. Zhang. 2004. Fluorescent indicators of cAMP and Epac activation reveal differential dynamics of cAMP signaling within discrete subcellular compartments. *Proc. Natl. Acad. Sci. USA.* 101:16513–16518. http://dx.doi.org/10.1073/pnas.0405973101

Feinstein, T.N., V.L. Wehbi, J.A. Ardura, D.S. Wheeler, S. Ferrandon, T.J. Gardella, and J.-P. Vilardaga. 2011. Retromer terminates the generation of cAMP by internalized PTH receptors. *Nat. Chem. Biol.* 7:278–284. http://dx.doi.org/10.1038/nchembio.545

Ferrandon, S., T.N. Feinstein, M. Castro, B. Wang, R. Bouley, J.T. Potts, T.J. Gardella, and J.P. Vilardaga. 2009. Sustained cyclic AMP production by parathyroid hormone receptor endocytosis. *Nat. Chem. Biol.* 5:734–742. http://dx.doi.org/10.1038/nchembio.206

Gainetdinov, R.R., R.T. Premont, L.M. Bohn, R.J. Lefkowitz, and M.G. Caron. 2004. Desensitization of G protein-coupled receptors and neuronal functions. *Annu. Rev. Neurosci.* 27:107–144. http://dx.doi.org/10.1146/annurev.neuro.27.070203.144206

Gilman, A.G. 1987. G proteins: transducers of receptor-generated signals. *Annu. Rev. Biochem.* 56:615–649. http://dx.doi.org/10.1146/annurev.bi.56.070187.003151

Han, S.-O., K. Xiao, J. Kim, J.-H. Wu, J.W. Wisler, N. Nakamura, N.J. Freedman, and S.K. Shenoy. 2012. MARCH2 promotes endocytosis and lysosomal sorting of carvedilol-bound β_2-adrenergic receptors. *J. Cell Biol.* 199:817–830. http://dx.doi.org/10.1083/jcb.201208192

Hanyaloglu, A.C., and M. von Zastrow. 2008. Regulation of GPCRs by endocytic membrane trafficking and its potential implications. *Annu. Rev. Pharmacol. Toxicol.* 48:537–568. http://dx.doi.org/10.1146/annurev.pharmtox.48.113006.094830

Hanyaloglu, A.C., E. McCullagh, and M. von Zastrow. 2005. Essential role of Hrs in a recycling mechanism mediating functional resensitization of cell signaling. *EMBO J.* 24:2265–2283. http://dx.doi.org/10.1038/sj.emboj.7600688

Harper, C.B., M.R. Popoff, A. McCluskey, P.J. Robinson, and F.A. Meunier. 2013. Targeting membrane trafficking in infection prophylaxis: dynamin inhibitors. *Trends Cell Biol.* 23:90–101. http://dx.doi.org/10.1016/j.tcb.2012.10.007

Hausdorff, W.P., M. Bouvier, B.F. O'Dowd, G.P. Irons, M.G. Caron, and R.J. Lefkowitz. 1989. Phosphorylation sites on two domains of the β_2-adrenergic receptor are involved in distinct pathways of receptor desensitization. *J. Biol. Chem.* 264:12657–12665.

Herskovits, J.S., C.C. Burgess, R.A. Obar, and R.B. Vallee. 1993. Effects of mutant rat dynamin on endocytosis. *J. Cell Biol.* 122:565–578. http://dx.doi.org/10.1083/jcb.122.3.565

Irannejad, R., J.C. Tomshine, J.R. Tomshine, M. Chevalier, J.P. Mahoney, J. Steyaert, S.G.F. Rasmussen, R.K. Sunahara, H. El-Samad, B. Huang, and M. von Zastrow. 2013. Conformational biosensors reveal GPCR signalling from endosomes. *Nature.* 495:534–538. http://dx.doi.org/10.1038/nature12000

Jean-Alphonse, F., S. Bowersox, S. Chen, G. Beard, M.A. Puthenveedu, and A.C. Hanyaloglu. 2014. Spatially restricted G protein-coupled receptor activity via divergent endocytic compartments. *J. Biol. Chem.* 289:3960–3977. http://dx.doi.org/10.1074/jbc.M113.526350

Kobilka, B.K. 1995. Amino and carboxyl terminal modifications to facilitate the production and purification of a G protein-coupled receptor. *Anal. Biochem.* 231:269–271. http://dx.doi.org/10.1006/abio.1995.1533

Lamb, M.E., W.F. De Weerd, and L.M. Leeb-Lundberg. 2001. Agonist-promoted trafficking of human bradykinin receptors: arrestin- and dynamin-independent sequestration of the B2 receptor and bradykinin in HEK293 cells. *Biochem. J.* 355:741–750. http://dx.doi.org/10.1042/bj3550741

Lefkowitz, R.J. 2007. Seven transmembrane receptors: something old, something new. *Acta Physiol. (Oxf.).* 190:9–19. http://dx.doi.org/10.1111/j.1365-201X.2007.01693.x

Lefkowitz, R.J., J. Pitcher, K. Krueger, and Y. Daaka. 1997. Mechanisms of β-adrenergic receptor desensitization and resensitization. *Adv. Pharmacol.* 42:416–420. http://dx.doi.org/10.1016/S1054-3589(08)60777-2

Liggett, S.B., M. Bouvier, W.P. Hausdorff, B. O'Dowd, M.G. Caron, and R.J. Lefkowitz. 1989. Altered patterns of agonist-stimulated cAMP accumulation in cells expressing mutant β_2-adrenergic receptors lacking phosphorylation sites. *Mol. Pharmacol.* 36:641–646.

Macia, E., M. Ehrlich, R. Massol, E. Boucrot, C. Brunner, and T. Kirchhausen. 2006. Dynasore, a cell-permeable inhibitor of dynamin. *Dev. Cell.* 10:839–850. http://dx.doi.org/10.1016/j.devcel.2006.04.002

Magalhaes, A.C., H. Dunn, and S.S.G. Ferguson. 2012. Regulation of GPCR activity, trafficking and localization by GPCR-interacting proteins. *Br. J. Pharmacol.* 165:1717–1736. http://dx.doi.org/10.1111/j.1476-5381.2011.01552.x

Marchese, A., M.M. Paing, B.R. Temple, and J. Trejo. 2008. G protein-coupled receptor sorting to endosomes and lysosomes. *Annu. Rev. Pharmacol. Toxicol.* 48:601–629. http://dx.doi.org/10.1146/annurev.pharmtox.48.113006.094646

Maxfield, F.R., and T.E. McGraw. 2004. Endocytic recycling. *Nat. Rev. Mol. Cell Biol.* 5:121–132. http://dx.doi.org/10.1038/nrm1315

Mayor, S., J.F. Presley, and F.R. Maxfield. 1993. Sorting of membrane components from endosomes and subsequent recycling to the cell surface occurs by a bulk flow process. *J. Cell Biol.* 121:1257–1269. http://dx.doi.org/10.1083/jcb.121.6.1257

McCluskey, A., J.A. Daniel, G. Hadzic, N. Chau, E.L. Clayton, A. Mariana, A. Whiting, N.N. Gorgani, J. Lloyd, A. Quan, et al. 2013. Building a better dynasore: the dyngo compounds potently inhibit dynamin and endocytosis. *Traffic.* 14:1272–1289. http://dx.doi.org/10.1111/tra.12119

Okamoto, T., Y. Murayama, Y. Hayashi, M. Inagaki, E. Ogata, and I. Nishimoto. 1991. Identification of a G_s activator region of the β2-adrenergic receptor that is autoregulated via protein kinase A-dependent phosphorylation. *Cell.* 67:723–730. http://dx.doi.org/10.1016/0092-8674(91)90067-9

Okazaki, M., S. Ferrandon, J.-P. Vilardaga, M.L. Bouxsein, J.T. Potts Jr., and T.J. Gardella. 2008. Prolonged signaling at the parathyroid hormone receptor by peptide ligands targeted to a specific receptor conformation. *Proc. Natl. Acad. Sci. USA.* 105:16525–16530. (Published erratum appears in *Proc. Natl. Acad. Sci. USA.* 105:20559) http://dx.doi.org/10.1073/pnas.0808750105

Pierce, K.L., R.T. Premont, and R.J. Lefkowitz. 2002. Seven-transmembrane receptors. *Nat. Rev. Mol. Cell Biol.* 3:639–650. http://dx.doi.org/10.1038/nrm908

Ponsioen, B., J. Zhao, J. Riedl, F. Zwartkruis, G. van der Krogt, M. Zaccolo, W.H. Moolenaar, J.L. Bos, and K. Jalink. 2004. Detecting cAMP-induced Epac activation by fluorescence resonance energy transfer: Epac as a novel cAMP indicator. *EMBO Rep.* 5:1176–1180. http://dx.doi.org/10.1038/sj.embor.7400290

Puthenveedu, M.A., B. Lauffer, P. Temkin, R. Vistein, P. Carlton, K. Thorn, J. Taunton, O.D. Weiner, R.G. Parton, and M. von Zastrow. 2010. Sequence-dependent sorting of recycling proteins by actin-stabilized endosomal microdomains. *Cell.* 143:761–773. http://dx.doi.org/10.1016/j.cell.2010.10.003

Romero, G., M. von Zastrow, and P.A. Friedman. 2011. Role of PDZ proteins in regulating trafficking, signaling, and function of GPCRs: means, motif, and opportunity. *Adv. Pharmacol.* 62:279–314. http://dx.doi.org/10.1016/B978-0-12-385952-5.00003-8

Seachrist, J.L., P.H. Anborgh, and S.S. Ferguson. 2000. β_2-adrenergic receptor internalization, endosomal sorting, and plasma membrane recycling are regulated by rab GTPases. *J. Biol. Chem.* 275:27221–27228.

Seibold, A., B. Williams, Z.F. Huang, J. Friedman, R.H. Moore, B.J. Knoll, and R.B. Clark. 2000. Localization of the sites mediating desensitization of the β_2-adrenergic receptor by the GRK pathway. *Mol. Pharmacol.* 58:1162–1173.

Soohoo, A.L., and M.A. Puthenveedu. 2013. Divergent modes for cargo-mediated control of clathrin-coated pit dynamics. *Mol. Biol. Cell.* 24:1725–1734. http://dx.doi.org/10.1091/mbc.E12-07-0550

Temkin, P., B. Lauffer, S. Jäger, P. Cimermancic, N.J. Krogan, and M. von Zastrow. 2011. SNX27 mediates retromer tubule entry and endosome-to-plasma membrane trafficking of signalling receptors. *Nat. Cell Biol.* 13:715–721. http://dx.doi.org/10.1038/ncb2252

Tsvetanova, N.G., and M. von Zastrow. 2014. Spatial encoding of cyclic AMP signaling specificity by GPCR endocytosis. *Nat. Chem. Biol.* 10:1061–1065. http://dx.doi.org/10.1038/nchembio.1665

Tsvetanova, N.G., R. Irannejad, and M. von Zastrow. 2015. G protein-coupled receptor (GPCR) signaling via heterotrimeric G proteins from endosomes. *J. Biol. Chem.* 290:6689–6696. http://dx.doi.org/10.1074/jbc.R114.617951

Vistein, R., and M.A. Puthenveedu. 2013. Reprogramming of G protein-coupled receptor recycling and signaling by a kinase switch. *Proc. Natl. Acad. Sci. USA.* 110:15289–15294. http://dx.doi.org/10.1073/pnas.1306340110

von Zastrow, M., and B.K. Kobilka. 1992. Ligand-regulated internalization and recycling of human β_2-adrenergic receptors between the plasma membrane and endosomes containing transferrin receptors. *J. Biol. Chem.* 267:3530–3538.

von Zastrow, M., and J.T. Williams. 2012. Modulating neuromodulation by receptor membrane traffic in the endocytic pathway. *Neuron.* 76:22–32. http://dx.doi.org/10.1016/j.neuron.2012.09.022

Werthmann, R.C., S. Volpe, M.J. Lohse, and D. Calebiro. 2012. Persistent cAMP signaling by internalized TSH receptors occurs in thyroid but not in HEK293 cells. *FASEB J.* 26:2043–2048. http://dx.doi.org/10.1096/fj.11-195248

West, C., and A.C. Hanyaloglu. 2015. Spatial programming of G protein-coupled receptor activity: decoding signaling in health and disease. *Mol. Endocrinol.* 29:1095–1106.

Westfield, G.H., S.G.F. Rasmussen, M. Su, S. Dutta, B.T. DeVree, K.Y. Chung, D. Calinski, G. Velez-Ruiz, A.N. Oleskie, E. Pardon, et al. 2011. Structural flexibility of the Gαs α-helical domain in the β_2-adrenoceptor Gs complex. *Proc. Natl. Acad. Sci. USA*. 108:16086–16091. http://dx.doi.org/10.1073/pnas.1113645108

Xiao, R.P. 2001. β-adrenergic signaling in the heart: dual coupling of the β_2-adrenergic receptor to G_s and G_i proteins. *Sci. STKE.*

Xiao, R.P., X. Ji, and E.G. Lakatta. 1995. Functional coupling of the β_2-adrenoceptor to a pertussis toxin-sensitive G protein in cardiac myocytes. *Mol. Pharmacol.* 47:322–329.

Yoburn, B.C., V. Purohit, K. Patel, and Q. Zhang. 2004. Opioid agonist and antagonist treatment differentially regulates immunoreactive mu-opioid receptors and dynamin-2 in vivo. *Eur. J. Pharmacol.* 498:87–96. http://dx.doi.org/10.1016/j.ejphar.2004.07.052

Yuan, N., J. Friedman, B.S. Whaley, and R.B. Clark. 1994. cAMP-dependent protein kinase and protein kinase C consensus site mutations of the β-adrenergic receptor. Effect on desensitization and stimulation of adenylylcyclase. *J. Biol. Chem.* 269:23032–23038.

Yudowski, G.A., M.A. Puthenveedu, A.G. Henry, and M. von Zastrow. 2009. Cargo-mediated regulation of a rapid Rab4-dependent recycling pathway. *Mol. Biol. Cell.* 20:2774–2784. http://dx.doi.org/10.1091/mbc.E08-08-0892

Zamah, A.M., M. Delahunty, L.M. Luttrell, and R.J. Lefkowitz. 2002. Protein kinase A-mediated phosphorylation of the β_2-adrenergic receptor regulates its coupling to G_s and G_i. Demonstration in a reconstituted system. *J. Biol. Chem.* 277:31249–31256. http://dx.doi.org/10.1074/jbc.M202753200